Oxidative capacity and radical chemistry in the polluted atmosphere of Hong Kong and Pearl River Delta region: analysis of a severe photochemical smog episode

Likun Xue[1*], Rongrong Gu[1], Tao Wang[2,1], Xinfeng Wang[1], Sandra Saunders[3], Donald Blake[4], Peter K. K. Louie[5], Connie W. Y. Luk[5], Isobel Simpson[4], Zheng Xu[1], Zhe Wang[2], Yuan Gao[2], Shuncheng Lee[2], Abdelwahid Mellouki[1], and Wenxing Wang[1]

[1] Environment Research Institute, Shandong University, Ji'nan, Shandong, China

[2] Department of Civil and Environmental Engineering, Hong Kong Polytechnic University, Hong Kong, China

[3] School of Chemistry and Biochemistry, University of Western Australia, WA, Australia

[4] Department of Chemistry, University of California at Irvine, Irvine, CA, USA

[5] Environmental Protection Department, the Government of Hong Kong Special Administrative Region, Hong Kong, China

[*]*To whom correspondence should be addressed*

E-mail: xuelikun@sdu.edu.cn, Tel: +86-531-8836 1185

Abstract

We analyze a photochemical smog episode to understand the oxidative capacity and radical chemistry of the polluted atmosphere in Hong Kong and the Pearl River Delta (PRD) region. A photochemical box model based on the Master Chemical Mechanism (MCM v3.2) is constrained by an intensive set of field observations to elucidate the budgets of RO_X ($RO_X=OH+HO_2+RO_2$) and NO_3 radicals. Highly abundant radical precursors (*i.e.,* O_3, HONO and carbonyls), nitrogen oxides (NO_X) and volatile organic compounds (VOCs) facilitate strong production and efficient recycling of RO_X radicals. The OH reactivity is dominated by oxygenated VOCs (OVOCs), followed by aromatics, alkenes and alkanes. Photolysis of OVOCs (except for formaldehyde) is the dominant primary source of RO_X with average daytime contributions of 34%–47%. HONO photolysis is the largest contributor to OH and the second most significant source (19%–22%) of RO_X. Other considerable RO_X sources include O_3 photolysis (11%–20%), formaldehyde photolysis (10%–16%), and ozonolysis reactions of unsaturated VOCs (3.9%–6.2%). In one case when solar irradiation was possibly attenuated by the high aerosol loadings, NO_3 became an important oxidant and the NO_3-initiated VOC oxidation presented another significant RO_X source (6.2%) even during daytime. This study suggests the possible impacts of daytime NO_3 chemistry in the polluted atmospheres under conditions with the co-existence of abundant O_3, NO_2, VOCs and aerosols, and also provides new insights into the radical chemistry that essentially drives the formation of photochemical smog in the high-NO_X environment of Hong Kong and the PRD

region.

1. Introduction

The hydroxyl radical (OH) and hydro/organic peroxy radicals (HO_2 and RO_2), collectively known as ROx, play a central role in atmospheric chemistry and air pollution (Stone et al., 2012). They dominate the oxidative capacity of atmosphere, and hence govern the removal of primary contaminants and formation of secondary pollutants such as ozone (O_3) and secondary organic aerosol (Hofzumahaus et al., 2009). In the troposphere, they arise from photolysis of closed-shell molecules such as O_3, nitrous acid (HONO), formaldehyde (HCHO) and other carbonyls, as well as ozonolysis reactions of unsaturated volatile organic compounds (VOCs) (Dusanter et al., 2009; Lu et al., 2012; Volkamer et al., 2010). In the presence of nitrogen oxides (NO_X) and VOCs, the RO_X radicals can undergo efficient recycling (*e.g.,* $OH \rightarrow RO_2 \rightarrow RO \rightarrow HO_2 \rightarrow OH$) and produce O_3 and oxygenated VOCs (OVOCs) (Sheehy et al., 2010). The radical recycling is terminated by their cross reactions with NO_X (under high-NO_X conditions) and RO_X themselves (under low-NO_X conditions), which results in the formation of nitric acid, organic nitrates and peroxides (Liu et al., 2012; Wood et al., 2009). Given the essential significance and complex processes involved, radical chemistry presents one of the core areas in the atmospheric chemistry research.

Understanding the sources and chemistry of RO_X has long been a focus of air quality studies over the past decades. It has been shown that although air pollution problems are visually quite similar, the radical chemistry, and in particular the relative importance of primary radical sources, is inhomogeneous in different metropolitan areas. For example, the dominant radical sources are O_3 photolysis in the South Coast Air Basin in California (2010 scenario) and Nashville, US (Martinez et al., 2003; Volkamer et al., 2010); HONO photolysis in New York City, US (Ren et al., 2003), Paris, France (Michoud et al., 2012) and Santiago, Chile (Elshorbany et al., 2009); HCHO photolysis in Milan, Italy (Alicke et al., 2002); and OVOC photolysis in Mexico City, Mexico (Volkamer et al., 2010), Beijing, China (Liu et al., 2012), Birmingham (summer scenario; Emmerson et al., 2005) and London in England (Emmerson et al., 2007) (note that HONO was not in-situ measured but simulated by a box model in Emmerson et al. (2005 and 2007), and hence the contributions of HONO photolysis might be underestimated). Therefore, identification of the principal radical sources is a fundamental step towards understanding the formation of air pollution and formulating science-based control strategies.

The nitrate radical (NO_3) is another important oxidant in the polluted atmosphere (Geyer et al., 2001). The NO_3-initiated degradation of VOCs presents an important source of RO_2, gaseous organic nitrates and nitrogen-containing aerosols (Rollins et al., 2012; Saunders et al., 2003). NO_3 has been recognized as a major player in nocturnal chemistry, but is usually neglected for the daytime chemistry given its fast photolysis in sunlight (Volkamer et al., 2010). Under certain conditions, *e.g.,* with abundant O_3 and NO_2 (hence strong NO_3 production) and weak solar radiation (thus weak photolysis),

however, NO_3 may also play a role in the daytime chemistry. Indeed, Geyer et al. (2003) observed by differential optical absorption spectroscopy (DOAS) ~5 pptv of NO_3 three hours before sunset in Houston, and indicated considerable contribution (10%) of NO_3 chemistry to the daytime O_X loss. More studies are required to confirm the possible operation of NO_3 chemistry during daytime and to evaluate its impacts on the atmospheric oxidative capacity (AOC) and formation of O_3 and secondary aerosols.

Hong Kong and the adjacent Pearl River Delta (PRD) is the most industrialized region of southern China, and is suffering from serious photochemical air pollution (e.g., Ling et al., 2014; Zheng et al., 2010). A number of studies have been conducted in the last decade, most of which focused on either O_3-precursor relationships (Zhang J. et al., 2007; Zhang Y. et al., 2008) or local vs. regional contributions (Wang et al., 2009; Li et al., 2012; Xue et al., 2014b), but few has attempted to understand the atmospheric oxidizing capacity and radical chemistry (Lu et al., 2014). Recent studies have observed the highest ever-reported concentrations of OH and HO_2 at a rural site in the northern PRD, which cannot be reproduced by the classic knowledge of atmospheric chemistry (Hofzumahaus et al., 2009). This indicates the strong oxidative capacity of atmosphere in this region as well as a deficiency in understanding the chemistry underlying the pollution.

As part of the Hong Kong Supersite programme aimed at elucidating the causes of regional smog and haze pollution, an intensive field campaign was conducted at a regional receptor site in summer 2011. A comprehensive set of measurements was taken, which facilitated the construction of a detailed observation-constrained box model to study the atmospheric photochemistry. In the present work, we analyze a severe photochemical episode occurring during 25–31 August 2011 to gain an understanding of atmospheric oxidative capacity and radical chemistry. We first provide an observational overview of the episode, and then evaluate the chemical budgets of both RO_X and NO_3 radicals. This study provides some new insights regarding: (1) the potential impact of NO_3 on the daytime photochemistry in polluted atmospheres and (2) the primary radical sources of RO_X in the high-NO_X environment of Hong Kong and the PRD region.

2. Methods

2.1. Experimental

The measurements were conducted at the Tung Chung air quality monitoring station (TC; 113.93 ° E, 22.30 ° N). It is located about 3 *km* south of the Hong Kong International airport, and is in a residential area of a new town in western Hong Kong (see *Fig. S1*). This station is characterized as a polluted receptor site as it receives urban plumes from Hong Kong under easterly winds and regional air masses from the PRD region when northerly winds prevail, and is the location where the maximum O_3 levels are usually recorded in Hong Kong (Xue et al., 2014b). Details of this station and analyses of HONO and aerosol data have been described in our previous publications (Xu et al., 2015; Xue et al.,

2014b; Zhou et al., 2014).

A one-month campaign was carried out from 6 August to 7 September 2011, which covered two distinct types of meteorological conditions and air quality (see *Fig. 1*). For the majority of the campaign, Hong Kong was influenced by clean marine air masses and featured by good air quality (typical summer conditions as a result of the Asian monsoon). In contrast from 25-31 August, a heavy multi-day photochemical smog event hit Hong Kong with northerly winds prevailing during the daytime and elevated concentrations of various air pollutants were observed. In the present study, this episode was subject to a detailed modeling analysis to understand the atmospheric oxidative capacity and RO_X chemistry, made possible with the most comprehensive suite of measurements taken for the first time in Hong Kong.

A full suite of trace gases and meteorological parameters were simultaneously measured during this episode (as summarized in *Table S1*). Here a brief description is given of the measurements used in the present study. Major air quality target pollutants were routinely monitored with commercial analyzers: O_3 with a UV photometric analyzer (*TEI model 49i*); CO with a non-dispersive infrared equipment (*API model 300EU*); NO and NO_2 with a chemiluminescence analyzer (*TEI model 42i*) equipped with a selective blue light converter (Xu et al., 2013). NO_y was measured by another chemiluminescence instrument (*TEI model 42cy*) with an external molybdenum oxide (MoO) catalytic converter (Xue et al., 2011). HONO was measured in real-time by a long path absorption photometer (*QUMA model LOPAP-03*) (Xu et al., 2015). Nitryl chloride ($ClNO_2$) was detected using a custom-built chemical ionization mass spectrometer (CIMS; *THS Instruments Inc., Atlanta*) (Tham et al., 2014). Peroxyacetyl nitrate (PAN) was measured by the same CIMS instrument with a heated inlet, and the potential interference caused by high NO was corrected based on laboratory tests (Slusher et al., 2004; Wang et al., 2014). Hydrogen peroxide (H_2O_2) and organic peroxides were measured by an enzyme-catalyzed fluorescence instrument (*Aerolaser AL-2021*) (Guo et al., 2014). Particle number and size distributions in the range of 5 nm – 10 μm, which were used to calculate the aerosol surface density, were measured with a wide range particle spectrometer (*WPS; MSP model 1000XP*) (Gao et al., 2009).

C_2-C_{10} non-methane hydrocarbons were measured at a time interval of 30 minutes by a commercial analyzer that combines gas chromatography (GC) with photoionization detection (PID) and flame-ionization detection (FID) (*Syntech Spectras, model GC955 Series 600/800 POCP*). The detection limits for the measured VOCs ranged from 0.001 to 0.19 ppbv. In addition, 24-hour whole air canister samples were collected on selected days (e.g., 25 and 29 August) for the detection of C_1-C_{10} hydrocarbons by using GC with FID, electron capture detection (ECD) and mass spectrometry detection (MSD). The analyses were carried out at the laboratory of the University of California at Irvine, and the detection limit was 3 pptv for all measured species (Simpson et al., 2010; Xue et al., 2013). As evaluated in our previous study, both sets of hydrocarbon measurements agree very well apart from the

alkenes. Here the real-time data tended to systematically overestimate the canister measurements (Xue et al., 2014b). Considering the generally lower detection limit of the canister observations, the high resolution real-time data were corrected in the present study according to the canister data. C_1-C_8 carbonyls were measured by collecting air samples on DNPH-coated sorbent cartridges followed by high pressure liquid chromatography analysis (Xue et al., 2014c). For the carbonyls, a 24-hour integrated sample was collected on 25 August, and eight 3-hour samples were taken throughout the day on 31 August. The measured hydrocarbon and carbonyl species are listed in *Table 1*.

Meteorological parameters were monitored by a series of commercial sensors, including a probe for ambient temperature and relative humidity (*Young RH/T probe*) and an ultrasonic sensor for wind speed and direction (*Gill WindSonic*). Photolysis frequency of NO$_2$ (J_{NO2}) was measured with a filter radiometer (*Meteorologie Consult gmbh*). All of the above techniques have been validated and applied in many previous studies, with detailed descriptions of the measurement principles, quality assurance and control procedures provided elsewhere (Guo et al., 2014; Xu et al., 2015; Xue et al., 2011, 2014a, 2014b and 2014c). See also *Table S1* for a summary of the measurement techniques/instruments and time resolutions.

2.2. The OBM-AOCP model

The zero-dimensional chemical box model OBM-AOCP (Observation-Based Model for investigating the Atmospheric Oxidative Capacity and Photochemistry) has been utilized in many previous studies to evaluate O$_3$ production (Xue et al., 2013, 2014a, 2014b), PAN formation (Xue et al., 2014c), and oxidative capacity (Xue et al., 2015). Briefly, the model is built on the Master Chemical Mechanism (MCM; v3.2), a nearly explicit gas phase mechanism describing the degradation of 143 primary VOCs (Jenkin et al., 2003; Saunders et al., 2003), and is updated to include both a heterogeneous chemistry scheme (including heterogeneous processes of NO$_2$, NO$_3$, N$_2$O$_5$, HO$_2$ and ClONO$_2$; Xue et al., 2014a) and a chlorine chemistry module that describes the reactions of Cl radical with various VOC compounds (Xue et al., 2015; note that the basic MCM only considers the reactions of Cl radical with alkanes). In addition to the chemistry, dry deposition and dilution mixing within the boundary layer are also included in the model (Xue et al., 2014a). The mixing layer height affecting the deposition rate and dilution mixing was assumed to vary from 300 m at night to 1500 m in the afternoon. Sensitivity model runs with different maximum mixing heights (1000 and 2000 m) indicated that its impacts on the modeling results (e.g., simulated HO$_X$ concentrations and OH production rate) were negligible. A detailed description of the model set up is provided in the supplementary materials.

The model is capable of simulating the concentrations of highly reactive species (*e.g.,* radicals) and quantitatively evaluating several key aspects of atmospheric photochemistry such as oxidant formation (*e.g.,* O$_3$ and PAN), VOC oxidation and radical budgets. In our model, the rates of over 15600 reactions out of the full MCM (v3.2) are individually and instantaneously computed and grouped into a relatively

small number of major routes. The calculation of ozone and PAN production rates have been described elsewhere (Xue et al., 2014a; 2014c). Here the emphasis is placed on the computation of AOC and RO_X budget. AOC is calculated as the sum of oxidation rates of CO and VOCs by the principal oxidants, namely OH, O_3, NO_3 and Cl (Xue et al., 2015). The partitioning of the AOC among individual oxidants or VOC groups can be also assessed. The chemical budgets of OH, HO_2 and RO_2 are quantified by grouping a huge number of relevant reactions into dozens of major production, cycling and loss routes. The principal radical sources in the polluted atmosphere generally include photolysis of O_3, HONO, H_2O_2 and OVOCs as well as reactions of O_3+VOCs, NO_3+VOCs and Cl+VOCs. The radical sinks mainly include the RO_X-NO_X and RO_X-RO_X cross reactions. Besides, a number of other minor reaction pathways were also computed to facilitate a thorough investigation of the RO_X chemistry (see *Figures 5 and 7*).

The measurement data of O_3, NO, NO_2, HONO, $ClNO_2$, H_2O_2, PAN, CO, C_1-C_{10} HCs, C_1-C_8 carbonyls, aerosol surface area and radius, temperature, RH and J_{NO2} were averaged or interpolated to a time resolution of 10 minutes for the model constraints. For carbonyls, the diurnal profiles measured on 31 August 2011, throughout which eight 3-hour samples were collected, were adopted and scaled to the 24-hour average data observed on 25 August (see *Figure S4* for the measured profiles of selected carbonyls). An initial concentration of 0.5 ppm of H_2 was assumed in the model. Photolysis frequencies were calculated as a function of solar zenith angle within the model (Saunders et al., 2003) and further scaled with the measured J_{NO2} values. The model starts from 00:00 local time and runs for a 24-hour period. Prior to the formal calculation, the model was run for five days with constraints of the campaign-average data to reach steady states for the unconstrained compounds (*e.g.,* radicals). The final outputs were extracted and subject to further analyses.

3. Results and Discussion

3.1. Observational overview

The measured concentrations of major pollutants and meteorological parameters at TC are depicted in *Figure 1*. During 25-31 August 2011, obviously, Hong Kong was hit by a prolonged photochemical smog episode, with concentrations of various air pollutants exceeding the ambient air quality standard (the zoomed-in figure of this episode is given in the supplementary materials). Peak O_3 mixing ratios of over 150 ppbv were observed almost every day within the 1-week period, except for 29 August when the peak was 135 ppbv. As another indicator of photochemical smog, the concentrations of PAN were also very high with the peak values exceeding 4 ppbv every day (except for 3.7 ppbv on 29 August). The maximum hourly values of O_3 and PAN were recorded at 162 and 6.95 ppbv, respectively. Extremely high levels of NO_X (peak of ~150 ppbv), CO (peak of ~1000 ppbv) and particulate matter (as indicative of >500 Mm^{-1} of aerosol scattering coefficient) were also determined. Overall, inspection of observational data reveals the markedly poor air quality and serious photochemical pollution over the

region during the episode.

Table 1 lists the 24-h average concentrations of hydrocarbons and carbonyls measured on 25 and 31 August 2011. It is clearly seen that the VOC levels, in particular for reactive aromatics and aldehydes, were also very high during the episode. On 25 August, for instance, the 24-h average values of toluene, summed xylenes, formaldehyde and acetaldehyde were as high as 9.47, 3.87, 9.89 and 4.25 ppbv, which were 3–30 folders higher than those measured during the non-episode period of the campaign (figures not shown). HONO and $ClNO_2$, two precursors of OH and Cl radicals, were also measured. Elevated HONO (up to 2–3 ppbv) and moderate $ClNO_2$ (up to 0.5–1 ppbv) were usually found at night, and what is more interesting is that the daytime HONO levels were also significant (over 1 ppbv in general; see *Fig. 1*). Such daytime HONO levels cannot be explained by the known gas-phase source and indicates the existence of other unknown source(s) (Xu et al., 2015), yet exploring the unknown HONO sources is beyond the scope of the present study. High abundances of O_3, HONO and carbonyls would definitely lead to strong production of RO_X radicals, and the abundant VOCs would facilitate efficient radical propagation (e.g., OH→RO_2). Therefore, strong atmospheric oxidative capacity and intensive *in-situ* photochemistry can be expected from the above analyses.

The dynamic cause of this episode was a distant tropical cyclone that introduced warm stagnant weather and facilitated accumulation of air pollutants in Hong Kong and the PRD region. The weather condition featured high temperatures (30 ℃–35 ℃) and relatively low RH (40%–80%; see *Fig. S2*). During the daytime, the prevailing surface winds were consistently from the northwest with relatively low wind speeds (~2 m/s), suggesting the transport of processed air masses from the upwind PRD region to the site. This was further confirmed by the 48-h backward trajectories calculated by the HYSPLIT model (Draxler and Rolph, 2016), which indicated that for most days the air masses had spent a large portion of time over the PRD region prior to arriving at TC (*Fig. S3*).

There was an exception on 25 August when the air flow was switching from southerly maritime air to northerly PRD regional air masses (see *Fig. S3*). This case is believed to be more influenced by the local air in Hong Kong, because (1) northerly winds during the daytime were somewhat weak compared to the other cases (see *Fig. S2*); (2) the backward trajectories also indicated less impact from the PRD region (*Fig. S3*); and (3) the CO/NO_y ratio on that day was significantly lower than those on the following days (*Fig. S5*), which is consistent with the previous finding that the PRD air masses have higher CO/NO_y ratios than those from Hong Kong (Wang et al., 2003). The evolution of the CO/NO_y ratio clearly indicates the transition from local (25 August) to regional air masses (27–31 August) throughout the 1-week episode (*Fig. S5*). In the following discussion, detailed modeling analyses are conducted for the 25 and 31 August cases, which are representative of local Hong Kong and regional PRD pollution, respectively.

3.2. Atmospheric oxidative capacity

The strong oxidative capacity of the atmosphere during the pollution episodes was confirmed by quantifying the loss rates of CO and VOCs via reactions with OH, O_3, NO_3 and Cl, as shown in *Fig. 2*. The calculated AOC was up to 2.04×10^8 and 1.27×10^8 molecules cm^{-3} s^{-1}, with daytime averages (6:00–18:00 LT) of 7.26×10^7 and 6.30×10^7 molecules cm^{-3} s^{-1}, on 25 and 31 August, respectively. As such, the total number of CO and VOC molecules depleted throughout the daytime was 3.14×10^{12} and 2.72×10^{12} per cm^{-3} of air for both cases. Such levels of AOC at TC are much higher than those determined from a rural site in Germany (Geyer et al., 2001), but a bit lower than that assessed from a polluted area in Santiago, Chile (Elshorbany et al., 2009).

OH was, as expected, the predominant oxidant accounting for 89% and 93% of the AOC on 25 and 31 August, respectively. NO_3 was the second important oxidant with contributions of 7% and 3% for both cases. In particular, NO_3 contributed to 43% of the AOC at 15:00 LT on 25 August under a weak solar radiation condition. The major fuels for NO_3 oxidation were OVOCs (i.e., 77%–90%) and alkenes (10%–23%). In comparison, O_3 and Cl (produced from $ClNO_2$ photolysis) had minor contributions due to the relatively lower abundances of alkenes and Cl radicals (i.e., the modeled peak value of Cl was $\sim 1 \times 10^4$ atoms/cm^3). Overall, the OH-dominated AOC at TC is in line with the previous studies at other urban locales (Elshorbany et al., 2009; Bannan et al., 2015), and the present analysis suggests that the NO_3 radical may play an important role in the daytime oxidation under certain conditions (see a detailed evaluation in Section 3.4).

We further assessed the loss rates of major VOC groups due to OH oxidation, by which the partitioning of OH reactivity among different VOCs can be elucidated. The results are presented in *Fig. 3*. OVOCs clearly dominate the OH reactivity with daytime average contributions of 60% and 75% and with maximums in the afternoon of over 80% for both cases. Aromatics are the second largest contributor comprising on average 22% and 10% of the daytime OH reactivity. For the Hong Kong local case on 25 August, especially, aromatics made up the majority (*i.e.,* 40%–60%) of the OH reactivity in the early morning period when there were much fresher air masses. In comparison, alkenes and alkanes only accounted for a small fraction (8%–10%) of the OH reactivity at TC. These results are in fair agreement with the previous studies of Lou et al. (2010) and Whalley et al. (2015), which indicated the dominance of secondary OVOCs in the observed OH reactivity in the PRD region and central London.

As shown above, the partitioning of principal oxidants and OH reactivity is quite similar for both cases. In comparison with the regional case on 31st August 2011, nonetheless, the Hong Kong local case (i.e., 25th August 2011) showed higher AOC levels and more contribution from aromatic VOCs to the OH reactivity. Such difference should be due to the fresher air masses and hence more reactive VOC species during the local case. In the following section, a detailed budget analysis of the radical initiation, recycling and termination processes is presented.

3.3.   RO$_X$ budget analysis

3.3.1.   The Hong Kong local case

Figure 4 presents the primary daytime sources of OH, HO$_2$ and RO$_2$ at TC on 25 August 2011, and the detailed daytime RO$_X$ budget is schematically illustrated in *Fig. 5*. HONO photolysis is not only the predominant source of OH in the early morning but also a major source throughout the daytime. Photolysis of O$_3$ becomes an important OH source at midday, the strength of which is comparable to that of HONO photolysis. In terms of the daytime average (6:00–18:00, LT), HONO photolysis is the dominant OH source with an average OH production rate of 1.5 ppbv/h, followed by O$_3$ photolysis (0.9 ppbv/h). In addition, ozonolysis reactions of unsaturated VOCs are another considerable OH source with a mean production rate of 0.2 ppbv/h, whilst other sources (*e.g.,* photolysis of H$_2$O$_2$, HNO$_3$ and OVOCs) are generally negligible.

For HO$_2$, the most important source is the photolysis of OVOCs (including not only the measured carbonyls but also the oxidation products generated within the model), with a daytime average production rate of 2.7 ppbv/h. Specifically, photolysis of formaldehyde produces HO$_2$ at a rate of 0.8 ppbv/h, while the remaining majority (1.9 ppbv/h) is from the photolysis of the other OVOCs. Such source strength of OVOC photolysis was comparable to those determined in the metropolitan areas of Beijing (Liu et al., 2012) and Mexico City (Volkamer et al., 2010). In addition, another source that needs to be considered is reactions of O$_3$ with unsaturated VOCs, which produce HO$_2$ at 0.1 ppbv/h on average during the daytime.

For RO$_2$, photolysis of OVOCs presents the dominant source with a daytime mean production rate of 1.9 ppbv/h. The NO$_3$ oxidation of VOCs is the second most significant RO$_2$ source at TC, contributing 0.5 ppbv/h of daytime RO$_2$ production. This result suggests that NO$_3$ may play an important role in the daytime chemistry of the polluted atmosphere, and is different from most results obtained elsewhere which have indicated the negligible role of NO$_3$ in the daytime photochemistry (Stone et al., 2012; and references therein; a detailed analysis is presented in Section 3.4). Ozonolysis reactions of VOCs also contribute moderately to the daytime RO$_2$ production (0.2 ppbv/h). Furthermore, oxidation of VOCs by the chlorine atoms, which are produced by photolysis of the nocturnally formed ClNO$_2$, is another RO$_2$ source (0.1 ppbv/h), particularly in the early morning period (with a maximum of 0.4 ppbv/h).

From the RO$_X$ perspective, the primary radical production in Hong Kong is dominated by photolysis of OVOCs (except for HCHO), followed by photolysis of HONO, O$_3$ and HCHO, and reactions of O$_3$+VOCs and NO$_3$+VOCs. Comparison of Hong Kong with other metropolitan areas clearly reveals the heterogeneity in radical chemistry in different urban environments. For example, the dominant radical sources are O$_3$ photolysis in Nashville (Martinez et al., 2003), HONO photolysis in

New York City (Ren et al., 2003), Paris (Michoud et al., 2012) and Santiago (Elshorbany et al., 2009), HCHO photolysis in Milan (Alicke et al., 2002), and OVOC photolysis in Hong Kong, Beijing (Liu et al., 2012), Mexico City (Volkamer et al., 2010), Birmingham (summer case; Emmerson et al., 2005) and Chelmsford near London (Emmerson et al., 2007). It is worth noting that HONO was not measured at Birmingham and Chelmsford but only simulated by a chemical box model, and thus the contributions of HONO photolysis were likely underestimated. The above analysis highlights the variability of the initiation mode of atmospheric photochemistry, which ultimately drives the formation of ozone and secondary aerosols in urban atmospheres.

Efficient recycling of radicals can be also illustrated in *Fig. 5*. Oxidation of CO and VOCs by OH produces HO_2 and RO_2 with daytime average rates of 3.3 and 8.0 ppbv/h, respectively. Reactions of RO_2+NO and HO_2+NO in turn result in strong production of RO (9.0 ppbv/h) and OH (12.5 ppbv/h), with O_3 formed as a by-product. It is evident that these recycling processes dominate the total production of OH, HO_2 and RO_2 radicals. It is common that the radical propagation is efficient and amplifies the effect of the newly-produced radicals in the polluted atmospheres with the co-existence of abundant NO_X and VOCs (Elshorbany et al., 2009; Liu et al., 2012). As to the termination processes, the RO_X radical sink is clearly dominated by their reactions with NO_X. Specifically, reactions of $OH+NO_2$ and RO_2+NO_2, forming HNO_3 and organic nitrates, contributed approximately 2.8 and 2.5 ppbv/h of the radical loss on daytime-average at TC. This is in line with the understanding that reactions with NO_X usually dominate the radical sink in high-NO_X environments.

3.3.2. The PRD regional case

The detailed radical budget for the regional case on 31st August 2011 is illustrated in *Figs.* 6 and 7. Overall, the chemical budget of RO_X radicals was essentially the same as that of the Hong Kong local case. Specifically, the most significant primary source is photolysis of OVOCs except for HCHO, which produces both HO_2 and RO_2 equally at a daytime average rate of 1.3 ppbv/h. The other important radical sources include photolysis of HONO (1.7 ppbv/h as OH), O_3 (1.5 ppbv/h as OH) and HCHO (1.2 ppbv/h as HO_2), ozonolysis reactions of unsaturated VOCs (0.3 ppbv/h for the sum of RO_X), and reactions of NO_3+VOCs (0.2 ppbv/h as RO_2) and $Cl+VOCs$ (0.1 ppbv/h as RO_2). For the termination processes, reactions of $OH+NO_2$ and RO_2+NO_2 present the major radical loss pathways, with daytime average rates of 3.5 and 1.5 ppbv/h respectively.

Despite the abovementioned general similarity, two aspects are noteworthy about the difference between the two cases. First, the primary radical source strength was significantly higher on 25th August than 31st August, suggesting the stronger oxidation capacity of the atmosphere during the local case. Second, the source strengths of photolysis of HONO, O_3 and HCHO were higher on 31st August than 25th August, whilst the sources of OVOCs photolysis, O_3+VOCs and NO_3+VOCs showed an opposite picture. Such difference in the partitioning of radical sources between both cases should be ascribed to

the higher VOC levels (with more fresh emissions) and weaker solar radiation (possibly attenuated by the high aerosol loading; see Section 3.4) on 25th August.

3.4. Evidence of daytime NO$_3$ chemistry

The NO$_3$ radical can initiate the oxidation of VOCs and lead to formation of RO$_2$ and nitrogen-containing organic aerosols (Rollins et al., 2012; Saunders et al., 2003). These processes are usually considered to mainly occur at night and be negligible during the daytime due to the fast photolysis of NO$_3$. In the present study, we observed an interesting case that provided evidence of the operation of daytime NO$_3$-initiated chemistry. The detailed measurement data of chemical and meteorological parameters in this case (*i.e.,* 25 August 2011) are depicted in *Fig. 8*. During this episode, the air was characterized by high concentrations of O$_3$ (up to 170 ppbv), NO$_2$ (~25 ppbv as the afternoon average) and VOCs (see *Table 1*). Meanwhile, the solar irradiation arriving at the surface was weaker than other days, as evidenced by the relatively lower values of J_{NO2} (with a peak of 6.0×10^{-3} s^{-1}) compared to clear days with $\sim 10 \times 10^{-3}$ s^{-1} (see *Fig. 1*). The ambient relative humidity (RH) in the afternoon was in the range of 60%-70%, implying that there was little cloud on the site, whilst the aerosol scattering coefficient was very high (up to 525 Mm^{-1}; compared to 28 ± 12 Mm^{-1} on clear days). Hence, the attenuated solar radiation is possibly attributed to the abundant aerosol loadings. Under such conditions, the model produced an afternoon peak of NO$_3$ of ~7 pptv at 13:30–15:00 LT (except for the maximum of 11.3 pptv at 14:50 LT that was coincident with an extremely low solar radiation condition).

To further understand the causes and impacts of the daytime NO$_3$ chemistry, a detailed budget analysis was conducted with the OBM-AOCP model. The midday average (9:00 – 15:00 LT) production and destruction rates of NO$_3$ from the individual reaction pathways are documented in *Fig. 9*. The co-existence of high concentrations of O$_3$ and NO$_2$ resulted in a very strong NO$_3$ production with an average strength of 11.0 ppb/h. Given its high reactivity, NO$_3$ once formed, can be readily photolysed as well as react with NO and VOCs. For this case, about 80% (*i.e.,* 8.8 ppb/h) of NO$_3$ reacted with NO to convert back to NO$_2$. Due to the weak solar radiation, photolysis only accounted for 6.2% (or 0.7 ppb/h) of the NO$_3$ loss. In comparison, reactions of NO$_3$ with VOCs contributed 11.7% (or 1.3 ppb/h) to the total loss at midday. During this episode, therefore, NO$_3$ appeared to be the second most important oxidant (see *Section 3.2*) and the reactions of NO$_3$ with VOCs presented a considerable RO$_2$ source during the daytime (*Section 3.3*). In addition, the NO$_3$-initiated degradation of VOCs could also lead to formation of secondary organic nitrate aerosols, but was not simulated in the present study.

The above analysis indicates the possible importance of NO$_3$-initiated oxidation in the daytime atmospheric photochemistry under specific conditions. This analysis is solely derived from an observation-based modeling study of a unique pollution case in Hong Kong. Nevertheless, we hypothesize that it may also take place in other polluted urban atmospheres, especially in the large cities of China. It is known that eastern China now suffers from widespread and severe photochemical smog

during the summer, which features by elevated concentrations of O_3, NO_X, VOCs, and fine particulate matter (Xue et al., 2014a). The intense air pollution usually induces 'smoldering' weather with poor visibility and hence attenuated solar irradiation (Ding et al., 2013). All these unfavorable conditions would facilitate the operation of daytime NO_3 chemistry as found in Hong Kong in the present study. Further studies are required to verify this phenomenon in other polluted environments and quantify its contributions to the formation of ozone and secondary organic aerosols.

4. Conclusions

The detailed atmospheric photochemistry during a severe smog episode in Hong Kong is analyzed. A strong oxidative capacity of the atmosphere is found and ascribed to OH and to a lesser extent NO_3. Elevated concentrations of O_3, NO_2, HONO and VOCs were concurrently observed, which resulted in strong production of RO_X and NO_3 as well as efficient radical recycling. Photolysis of OVOCs other than HCHO was found to be the dominant primary RO_X source, followed by photolysis of HONO, O_3 and HCHO, and reactions of O_3+VOCs and NO_3+VOCs. Higher AOC levels and stronger primary production of radicals were determined during the Hong Kong local case compared to the PRD regional case. Although the primary radical sources were essentially the same, photolysis of OVOCs (except for HCHO) and reactions of O_3+VOCs and NO_3+VOCs were stronger for the Hong Kong local case, which was ascribed to the higher VOC levels. In comparison, the source strengths of photolysis of HONO, O_3 and HCHO were higher during the regional case.

On 25 August 2011, a unique case when heavy air pollution attenuated the solar irradiation reaching the surface in Hong Kong, NO_3 was identified as an important oxidant in the daytime chemistry. VOC oxidation by NO_3 represented the second largest source of RO_2, with a daytime average production rate of 0.5 ppbv/h. The NO_3-initiated degradation of VOCs would enhance the formation of O_3 and nitrogen-containing organic aerosols. This study indicates the potential operation of the daytime NO_3 chemistry in polluted urban atmospheres characterized by the co-existence of abundant O_3, NO_2, VOCs and particles. Further studies, especially direct observations of the NO_3 radical, are required to verify this interesting phenomenon in other environments and to evaluate its contribution to the O_3 and secondary organic aerosol formation.

Acknowledgements

The authors appreciate Steven Poon, Yee Jun Tham, Shengzhen Zhou, Wei Nie and Jia Guo for their contributions to the field study; the University of Leeds for providing the Master Chemical Mechanism; and the NOAA Air Resources Laboratory for providing the web-based HYSPLIT model. We thank the two anonymous referees for their helpful comments to improve the quality of our original manuscript. The field observations were funded by the Environment and Conservation Fund of Hong Kong (project No.: 7/2009), and the data analyses were supported by the National Natural Science

Foundation of China (project No.: 41505111) and Qilu Youth Talent Programme of Shandong University.

Disclaimer

References

Alicke, B., Platt, U., and Stutz, J.: Impact of nitrous acid photolysis on the total hydroxyl radical budget during the Limitation of Oxidant Production/Pianura Padana Produzione di Ozono study in Milan, *J Geophys Res-Atmos*, 107, 2002.

Bannan, T. J., Booth, A. M., Bacak, A, Muller, J. B. A., Leather, K. E., Breton, M. L., Jones, B., Young, D., Coe, H., Allan, J., Visser, S., Slowik, J. G., Furger, M., Prévôt, A. S. H., Lee, J., Dunmore, R. E., Hopkins, J. R., Hamilton, J. F., Lewis, A. C., Whalley, L. K., Sharp, T., Stone, D., Heard, D. E., Fleming, Z. L., Leigh, R., Shallcross, D. E., and Percival, C. J.: The first UK measurements of nitryl chloride using a chemical ionization mass spectrometer in central London in the summer of 2012, and an investigation of the role of Cl atom oxidation, *J Geophys Res-Atmos*, 5638-5657, 2015.

Ding, A. J., Fu, C. B., Yang, X. Q., Sun, J. N., Petaja, T., Kerminen, V. M., Wang, T., Xie, Y., Herrmann, E., Zheng, L. F., Nie, W., Liu, Q., Wei, X. L., and Kulmala, M.: Intense atmospheric pollution modifies weather: a case of mixed biomass burning with fossil fuel combustion pollution in eastern China, *Atmos Chem Phys*, 13, 10545-10554, 2013.

Draxler, R. R. and Rolph, G. D.: HYSPLIT (HYbrid Single-Particle Lagrangian Integrated Trajectory) Model access via NOAA ARL READY Website (http://ready.arl.noaa.gov/ HYSPLIT.php). NOAA Air Resources Laboratory, Silver Spring, MD, 2016.

Dusanter, S., Vimal, D., Stevens, P. S., Volkamer, R., Molina, L. T., Baker, A., Meinardi, S., Blake, D., Sheehy, P., Merten, A., Zhang, R., Zheng, J., Fortner, E. C., Junkermann, W., Dubey, M., Rahn, T., Eichinger, B., Lewandowski, P., Prueger, J., and Holder, H.: Measurements of OH and HO_2 concentrations during the MCMA-2006 field campaign - Part 2: Model comparison and radical budget, *Atmos Chem Phys*, 9, 6655-6675, 2009.

Elshorbany, Y. F., Kurtenbach, R., Wiesen, P., Lissi, E., Rubio, M., Villena, G., Gramsch, E., Rickard, A. R., Pilling, M. J., and Kleffmann, J.: Oxidation capacity of the city air of Santiago, Chile, *Atmos Chem Phys*, 9, 2257-2273, 2009.

Emmerson, K. M., Carslaw, N., and Pilling, M. J.: Urban atmospheric chemistry during the PUMA campaign 2: Radical budgets for OH, HO_2 and RO_2, *J Atmos Chem*, 52, 165-183, 2005.

Emmerson, K. M., Carslaw, N., Carslaw, D. C., Lee, J. D., McFiggans, G., Bloss, W. J., Gravestock, T.,

Heard, D. E., Hopkins, J., Ingham, T., Pilling, M. J., Smith, S. C., Jacob, M., and Monks, P. S.: Free radical modelling studies during the UK TORCH Campaign in Summer 2003, *Atmos Chem Phys*, 7, 167-181, 2007.

Gao, J., Wang, T., Zhou, X. H., Wu, W. S., and Wang, W. X.: Measurement of aerosol number size distributions in the Yangtze River delta in China: Formation and growth of particles under polluted conditions, *Atmos Environ*, 43, 829-836, 2009.

Geyer, A., Alicke, B., Konrad, S., Schmitz, T., Stutz, J., and Platt, U.: Chemistry and oxidation capacity of the nitrate radical in the continental boundary layer near Berlin, *J Geophys Res-Atmos*, 106, 8013-8025, 2001.

Geyer, A., Alicke, B., Ackermann, R., Martinez, M., Harder, H., Brune, W., di Carlo, P., Williams, E., Jobson, T., Hall, S., Shetter, R., and Stutz, J.: Direct observations of daytime NO_3: Implications for urban boundary layer chemistry, *J Geophys Res-Atmos*, 108, 2003.

Guo, J., Tilgner, A., Yeung, C., Wang, Z., Louie, P. K. K., Luk, C. W. Y., Xu, Z., Yuan, C., Gao, Y., Poon, S., Herrmann, H., Lee, S., Lam, K. S., and Wang, T.: Atmospheric Peroxides in a Polluted Subtropical Environment: Seasonal Variation, Sources and Sinks, and Importance of Heterogeneous Processes, *Environ Sci Technol*, 48, 1443-1450, 2014.

Hofzumahaus, A., Rohrer, F., Lu, K. D., Bohn, B., Brauers, T., Chang, C. C., Fuchs, H., Holland, F., Kita, K., Kondo, Y., Li, X., Lou, S. R., Shao, M., Zeng, L. M., Wahner, A., and Zhang, Y. H.: Amplified Trace Gas Removal in the Troposphere, *Science*, 324, 1702-1704, 2009.

Jenkin, M. E., Saunders, S. M., Wagner, V., and Pilling, M. J.: Protocol for the development of the Master Chemical Mechanism, MCM v3 (Part B): tropospheric degradation of aromatic volatile organic compounds, *Atmos Chem Phys*, 3, 181-193, 2003.

Li, Y., Lau, A. K. H., Fung, J. C. H., Zheng, J. Y., Zhong, L. J., and Louie, P. K. K.: Ozone source apportionment (OSAT) to differentiate local regional and super-regional source contributions in the Pearl River Delta region, China, *J Geophys Res-Atmos*, 117, 2012.

Ling, Z. H., Guo, H., Lam, S. H. M., Saunders, S. M., and Wang, T.: Atmospheric photochemical reactivity and ozone production at two sites in Hong Kong: Application of a Master Chemical Mechanism-photochemical box model, *J Geophys Res-Atmos*, 119, 2014.

Liu, Z., Wang, Y., Gu, D., Zhao, C., Huey, L. G., Stickel, R., Liao, J., Shao, M., Zhu, T., Zeng, L., Amoroso, A., Costabile, F., Chang, C. C., and Liu, S. C.: Summertime photochemistry during CAREBeijing-2007: ROx budgets and O_3 formation, *Atmos Chem Phys*, 12, 7737-7752, 2012.

Lou, S., Holland, F., Rohrer, F., Lu, K., Bohn, B., Brauers, T., Chang, C. C., Fuchs, H., Haseler, R., Kita, K., Kondo, Y., Li, X., Shao, M., Zeng, L., Wahner, A., Zhang, Y., Wang, W., and Hofzumahaus, A.: Atmospheric OH reactivities in the Pearl River Delta - China in summer 2006: measurement and model results, *Atmos Chem Phys*, 10, 11243-11260, 2010.

Lu, K. D., Rohrer, F., Holland, F., Fuchs, H., Bohn, B., Brauers, T., Chang, C. C., Haseler, R., Hu, M.,

Kita, K., Kondo, Y., Li, X., Lou, S. R., Nehr, S., Shao, M., Zeng, L. M., Wahner, A., Zhang, Y. H., and Hofzumahaus, A.: Observation and modelling of OH and HO_2 concentrations in the Pearl River Delta 2006: a missing OH source in a VOC rich atmosphere, *Atmos Chem Phys*, 12, 1541-1569, 2012.

Lu, K. D., Rohrer, F., Holland, F., Fuchs, H., Brauers, T., Oebel, A., Dlugi, R., Hu, M., Li, X., Lou, S. R., Shao, M., Zhu, T., Wahner, A., Zhang, Y. H., and Hofzumahaus, A.: Nighttime observation and chemistry of HOx in the Pearl River Delta and Beijing in summer 2006, *Atmos Chem Phys*, 14, 4979-4999, 2014.

Martinez, M., Harder, H., Kovacs, T. A., Simpas, J. B., Bassis, J., Lesher, R., Brune, W. H., Frost, G. J., Williams, E. J., Stroud, C. A., Jobson, B. T., Roberts, J. M., Hall, S. R., Shetter, R. E., Wert, B., Fried, A., Alicke, B., Stutz, J., Young, V. L., White, A. B., and Zamora, R. J.: OH and HO_2 concentrations, sources, and loss rates during the Southern Oxidants Study in Nashville, Tennessee, summer 1999, *J Geophys Res-Atmos*, 108, 2003.

Michoud, V., Kukui, A., Camredon, M., Colomb, A., Borbon, A., Miet, K., Aumont, B., Beekmann, M., Durand-Jolibois, R., Perrier, S., Zapf, P., Siour, G., Ait-Helal, W., Locoge, N., Sauvage, S., Afif, C., Gros, V., Furger, M., Ancellet, G., and Doussin, J. F.: Radical budget analysis in a suburban European site during the MEGAPOLI summer field campaign, *Atmos Chem Phys*, 12, 11951-11974, 2012.

Ren, X. R., Harder, H., Martinez, M., Lesher, R. L., Oliger, A., Simpas, J. B., Brune, W. H., Schwab, J. J., Demerjian, K. L., He, Y., Zhou, X. L., and Gao, H. G.: OH and HO_2 chemistry in the urban atmosphere of New York City, *Atmos Environ*, 37, 3639-3651, 2003.

Rollins, A. W., Browne, E. C., Min, K. E., Pusede, S. E., Wooldridge, P. J., Gentner, D. R., Goldstein, A. H., Liu, S., Day, D. A., Russell, L. M., and Cohen, R. C.: Evidence for NOx Control over Nighttime SOA Formation, *Science*, 337, 1210-1212, 2012.

Saunders, S. M., Jenkin, M. E., Derwent, R. G., and Pilling, M. J.: Protocol for the development of the Master Chemical Mechanism, MCM v3 (Part A): tropospheric degradation of non-aromatic volatile organic compounds, *Atmos Chem Phys*, 3, 161-180, 2003.

Sheehy, P. M., Volkamer, R., Molina, L. T., and Molina, M. J.: Oxidative capacity of the Mexico City atmosphere - Part 2: A ROx radical cycling perspective, *Atmos Chem Phys*, 10, 6993-7008, 2010.

Simpson, I. J., Blake, N. J., Barletta, B., Diskin, G. S., Fuelberg, H. E., Gorham, K., Huey, L. G., Meinardi, S., Rowland, F. S., Vay, S. A., Weinheimer, A. J., Yang, M., and Blake, D. R.: Characterization of trace gases measured over Alberta oil sands mining operations: 76 speciated C_2-C_{10} volatile organic compounds (VOCs), CO_2, CH_4, CO, NO, NO_2, NOy, O_3 and SO_2, *Atmos Chem Phys*, 10, 11931-11954, 2010.

Slusher, D. L., Huey, L. G., Tanner, D. J., Flocke, F. M., and Roberts, J. M.: A thermal dissociation-chemical ionization mass spectrometry (TD-CIMS) technique for the simultaneous measurement of peroxyacyl nitrates and dinitrogen pentoxide, *J Geophys Res-Atmos*, 109, 2004.

Stone, D., Whalley, L. K., and Heard, D. E.: Tropospheric OH and HO_2 radicals: field measurements

and model comparisons, *Chem Soc Rev*, 41, 6348-6404, 2012.

Tham, Y. J., Yan, C., Xue, L. K., Zha, Q. Z., Wang, X. F., and Wang, T.: Presence of high nitryl chloride in Asian coastal environment and its impact on atmospheric photochemistry, *Chinese Sci Bull*, 59, 356-359, 2014.

Volkamer, R., Sheehy, P., Molina, L. T., and Molina, M. J.: Oxidative capacity of the Mexico City atmosphere - Part 1: A radical source perspective, *Atmos Chem Phys*, 10, 6969-6991, 2010.

Wang, T., Poon, C. N., Kwok, Y. H., and Li, Y. S.: Characterizing the temporal variability and emission patterns of pollution plumes in the Pearl River Delta of China, *Atmos Environ*, 37, 3539-3550, 2003.

Wang, T., Wei, X. L., Ding, A. J., Poon, C. N., Lam, K. S., Li, Y. S., Chan, L. Y., and Anson, M.: Increasing surface ozone concentrations in the background atmosphere of Southern China, 1994–2007, *Atmos. Chem. Phys.,* 9, 6217-6227, 2009.

Wang, X., Wang, T., Yan, C., Tham, Y. J., Xue, L., Xu, Z., and Zha, Q.: Large daytime signals of N_2O_5 and NO_3 inferred at 62 amu in a TD-CIMS: chemical interference or a real atmospheric phenomenon?, *Atmos Meas Tech*, 7, 1-12, 2014.

Whalley, L. K., Stone, D., Bandy, B., Dunmore, R., Hamilton, J. F., Hopkins, J., Lee, J. D., Lewis, A. C., and Heard, D. E.: Atmospheric OH reactivity in central London: observations, model predictions and estimates of in situ ozone production, *Atmos Chem Phys*, 16, 2109–2122, 2016.

Wood, E. C., Herndon, S. C., Onasch, T. B., Kroll, J. H., Canagaratna, M. R., Kolb, C. E., Worsnop, D. R., Neuman, J. A., Seila, R., Zavala, M., and Knighton, W. B.: A case study of ozone production, nitrogen oxides, and the radical budget in Mexico City, *Atmos Chem Phys*, 9, 2499-2516, 2009.

Xu, Z., Wang, T., Xue, L. K., Louie, P. K. K., Luk, C. W. Y., Gao, J., Wang, S. L., Chai, F. H., and Wang, W. X.: Evaluating the uncertainties of thermal catalytic conversion in measuring atmospheric nitrogen dioxide at four differently polluted sites in China, *Atmos Environ*, 76, 221-226, 2013.

Xu, Z., Wang, T., Wu, J. Q., Xue, L. K., Chan, J., Zha, Q. Z., Zhou, S. Z., Louie, P. K. K., and Luk, C. W. Y.: Nitrous acid (HONO) in a polluted subtropical atmosphere: Seasonal variability, direct vehicle emissions and heterogeneous production at ground surface, *Atmos Environ*, 106, 100-109, 2015.

Xue, L. K., Wang, T., Zhang, J. M., Zhang, X. C., Deliger, Poon, C. N., Ding, A. J., Zhou, X. H., Wu, W. S., Tang, J., Zhang, Q. Z., and Wang, W. X.: Source of surface ozone and reactive nitrogen speciation at Mount Waliguan in western China: New insights from the 2006 summer study, *J Geophys Res-Atmos*, 116, 2011.

Xue, L. K., Wang, T., Guo, H., Blake, D. R., Tang, J., Zhang, X. C., Saunders, S. M., and Wang, W. X.: Sources and photochemistry of volatile organic compounds in the remote atmosphere of western China: results from the Mt. Waliguan Observatory, *Atmos Chem Phys*, 13, 8551-8567, 2013.

Xue, L. K., Wang, T., Gao, J., Ding, A. J., Zhou, X. H., Blake, D. R., Wang, X. F., Saunders, S. M., Fan, S. J., Zuo, H. C., Zhang, Q. Z., and Wang, W. X.: Ground-level ozone in four Chinese cities: precursors, regional transport and heterogeneous processes, *Atmos Chem Phys*, 14, 13175-13188,

2014a.

Xue, L. K., Wang, T., Louie, P. K. K., Luk, C. W. Y., Blake, D. R., and Xu, Z.: Increasing External Effects Negate Local Efforts to Control Ozone Air Pollution: A Case Study of Hong Kong and Implications for Other Chinese Cities, *Environ Sci Technol*, 48, 10769-10775, 2014b.

Xue, L. K., Wang, T., Wang, X. F., Blake, D. R., Gao, J., Nie, W., Gao, R., Gao, X. M., Xu, Z., Ding, A. J., Huang, Y., Lee, S. C., Chen, Y. Z., Wang, S. L., Chai, F. H., Zhang, Q. Z., and Wang, W. X.: On the use of an explicit chemical mechanism to dissect peroxy acetyl nitrate formation, *Environ Pollut*, 195, 39-47, 2014c.

Xue, L. K., Saunders, S. M., Wang, T., Gao, R., Wang, X. F., Zhang, Q. Z., and Wang, W. X.: Development of a chlorine chemistry module for the Master Chemical Mechanism, *Geosci Model Dev*, 8, 3151-3162, 2015.

Zhang, J., Wang, T., Chameides, W. L., Cardelino, C., Kwok, J., Blake, D. R., Ding, A., and So, K. L.: Ozone production and hydrocarbon reactivity in Hong Kong, Southern China, *Atmos Chem Phys*, 7, 557-573, 2007.

Zhang, Y. H., Su, H., Zhong, L. J., Cheng, Y. F., Zeng, L. M., Wang, X. S., Xiang, Y. R., Wang, J. L., Gao, D. F., Shao, M., Fan, S. J., and Liu, S. C.: Regional ozone pollution and observation-based approach for analyzing ozone-precursor relationship during the PRIDE-PRD2004 campaign, *Atmos Environ*, 42, 6203-6218, 2008.

Zheng, J. Y., Zhong, L. J., Wang, T., Louie, P. K. K., and Li, Z. C.: Ground-level ozone in the Pearl River Delta region: Analysis of data from a recently established regional air quality monitoring network, *Atmos Environ*, 44, 814-823, 2010.

Zhou, S. Z., Wang, T., Wang, Z., Li, W. J., Xu, Z., Wang, X. F., Yuan, C., Poon, C. N., Louie, P. K. K., Luk, C. W. Y., and Wang, W. X.: Photochemical evolution of organic aerosols observed in urban plumes from Hong Kong and the Pearl River Delta of China, *Atmos Environ*, 88, 219-229, 2014.

Table 1. 24-hour average concentrations of hydrocarbons and oxygenated VOCs measured at Tung Chung on 25 and 31 August 2011.[a]

Species	25 August	31 August	Species	25 August	31 August
methane	2.264	2.275	benzene	1008	569
ethane	1192	525	toluene	9465	3557
propane	2717	1589	ethylbenzene	1718	700
n-butane	3751	1361	*o*-xylene	979	328
i-butane	2614	929	*m*-xylene	2082	935
n-pentane	1175	561	*p*-xylene	813	239
i-pentane	1569	817	propylbenzene	63	24
n-hexane	1161	1039	*i*-propylbenzene	54	20
n-heptane	519	297	*o*-ethyltoluene	140	82
n-octane	150	410	*m*-ethyltoluene	338	167
n-nonane	133	-	*p*-ethyltoluene	143	113
2-methylpentane	1123	-	*1,2,3*-trimethylbenzene	204	46
3-methylpentane	842	-	*1,2,4*-trimethylbenzene	515	338
ethene	1861	681	*1,3,5*-trimethylbenzene	124	49
propene	537	482	formaldehyde	9890	8968
1-butene	196	136	acetaldehyde	4250	3990
i-butene	224	282	propanal	940	670
trans-2-butene	68	36	acetone	590	10670
cis-2-butene	54	23	butanal	640	269
1,3-butadiene	72	57	pentanal	1420	1596
1-pentene	50	16	hexanal	200	506
Isoprene	779	65	benzaldehyde	890	660
α-pinene	92	48	methyl ethyl ketone	260	1027
β-pinene	36	21	acrolein	30	BDL
ethyne	2903	265	crotonaldehyde	30	510

[a] The units are pptv except for methane which is in ppmv. "-" indicates no data available, and "BDL" indicates below detection limit.
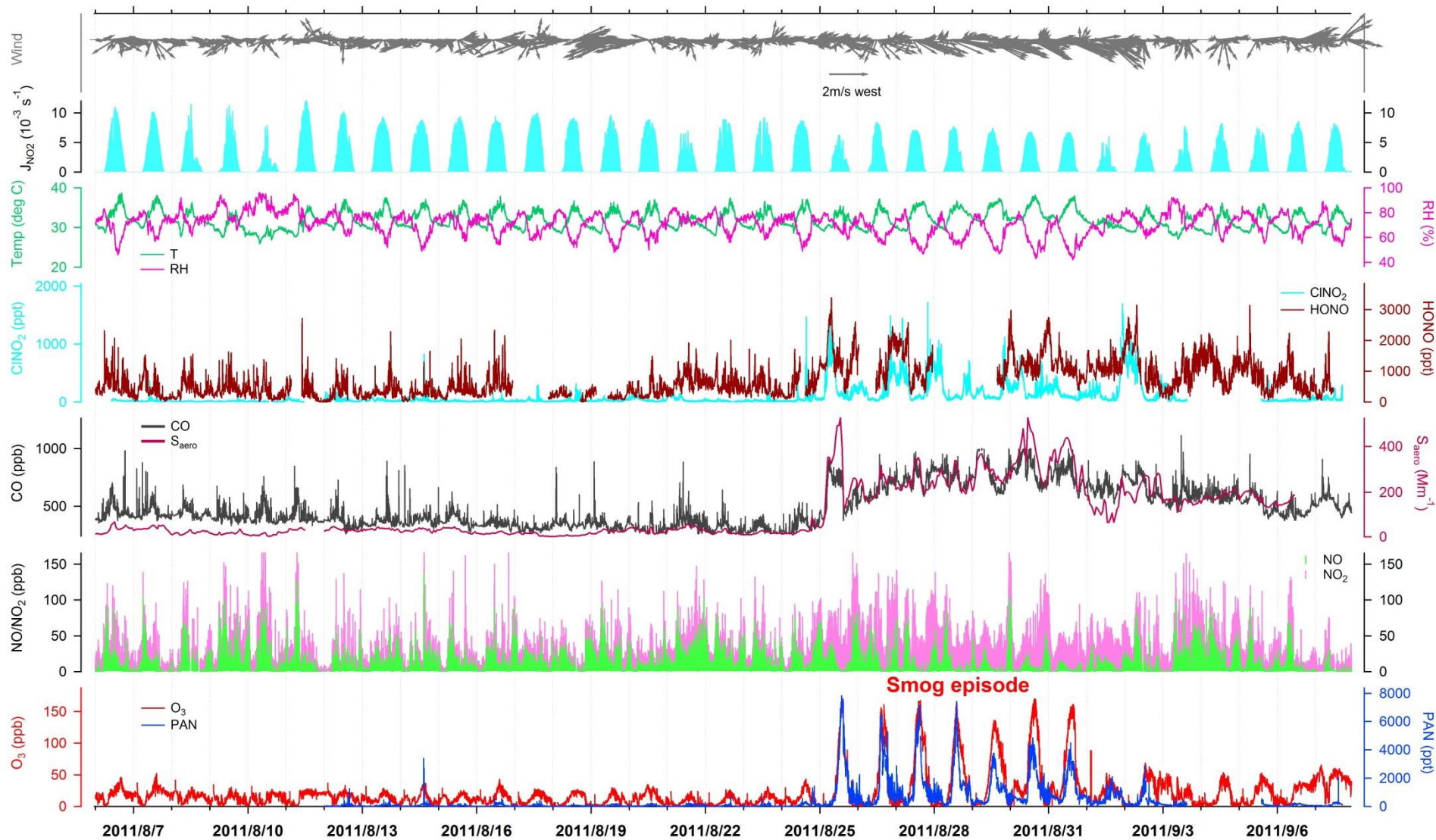
Figure 1. Time series of air pollutants and meteorological parameters observed at Tung Chung from 6 August to 7 September 2011. S_{aero} stands for the scattering coefficient of $PM_{2.5}$. The data gaps were mainly due to the calibration and maintenance of the instruments.
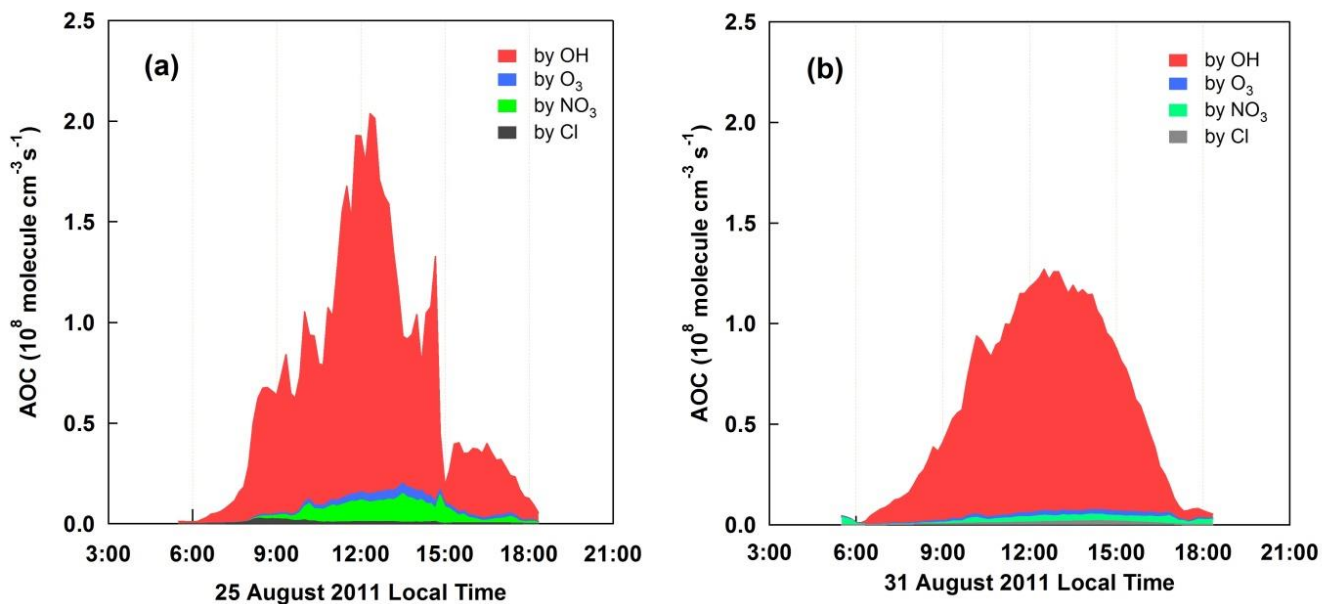
Figure 2. Daytime atmospheric oxidative capacity (AOC) and contributions of major oxidants at Tung Chung on (a) 25 August 2011 and (b) 31 August 2011.
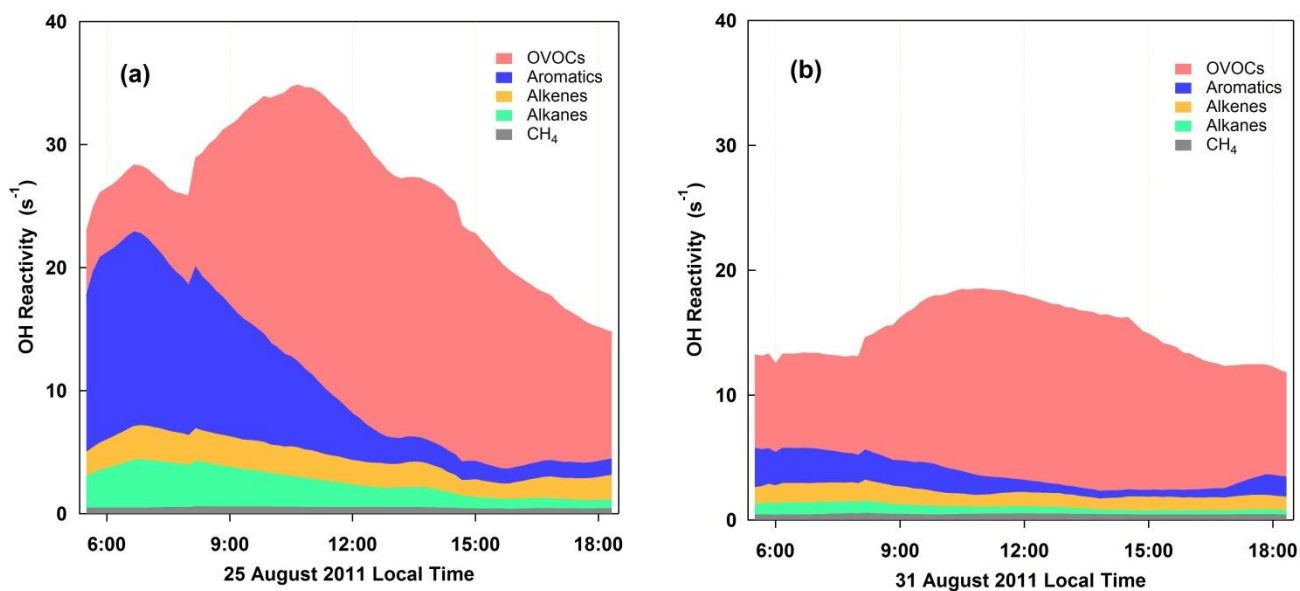
Figure 3. Partitioning of the daytime OH reactivity by oxidation of major VOC groups at Tung Chung on (a) 25 August 2011 and (b) 31 August 2011.
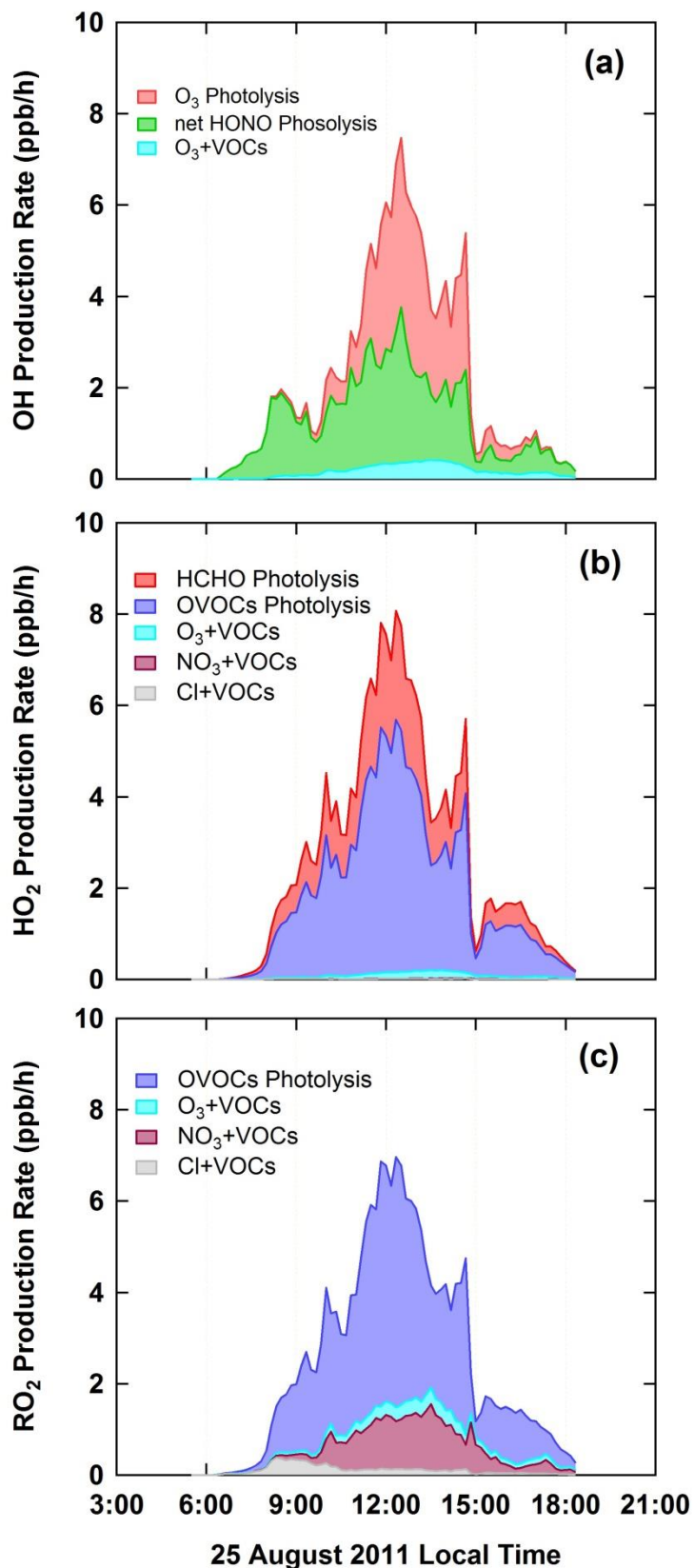
Figure 4. Primary daytime sources of (a) OH, (b) HO_2 and (c) RO_2 radicals at Tung Chung on 25 August 2011. The term "net HONO photolysis" represents the contribution of net HONO (i.e., subtracting the formation rate of HONO from NO + OH = HONO).
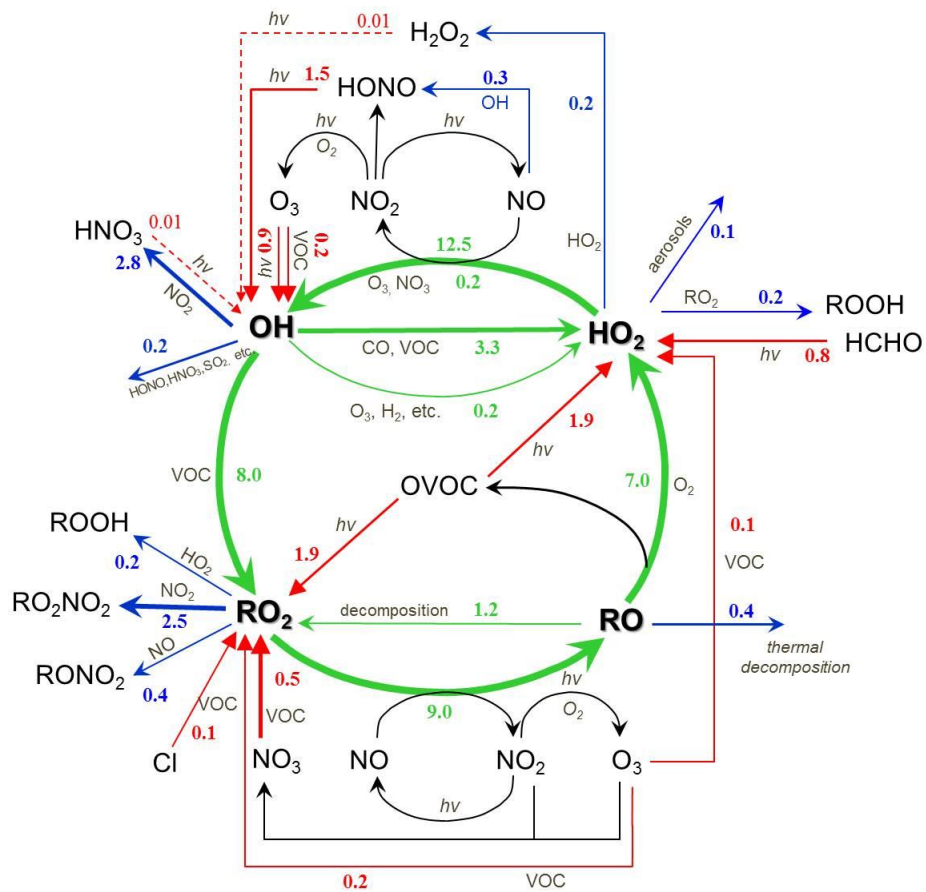
Figure 5. Daytime average RO$_X$ budget at Tung Chung on 25 August 2011. The unit is ppb/h. The red, blue and green lines indicate the production, destruction and recycling pathways of radicals, respectively.
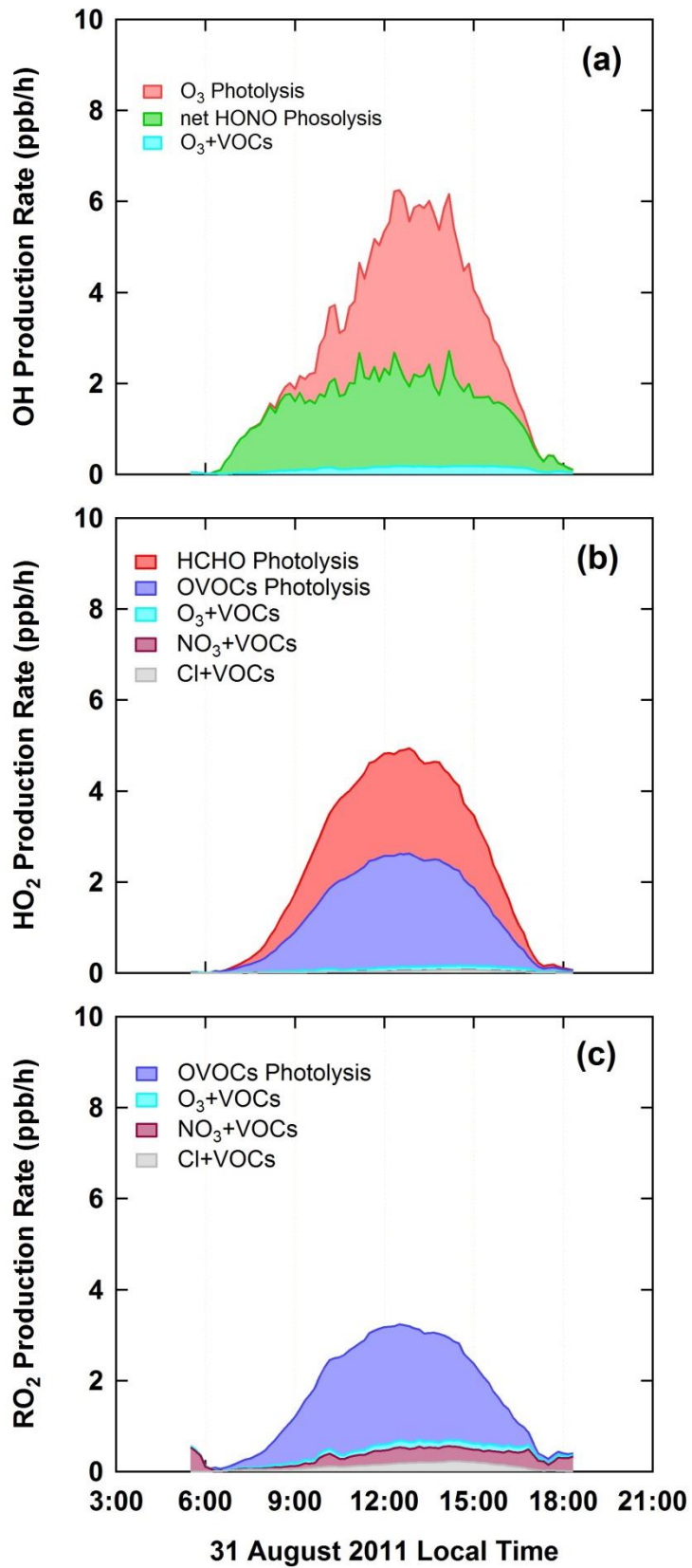
Figure 6. The same as Figure 4 but for the case of 31 August 2011.
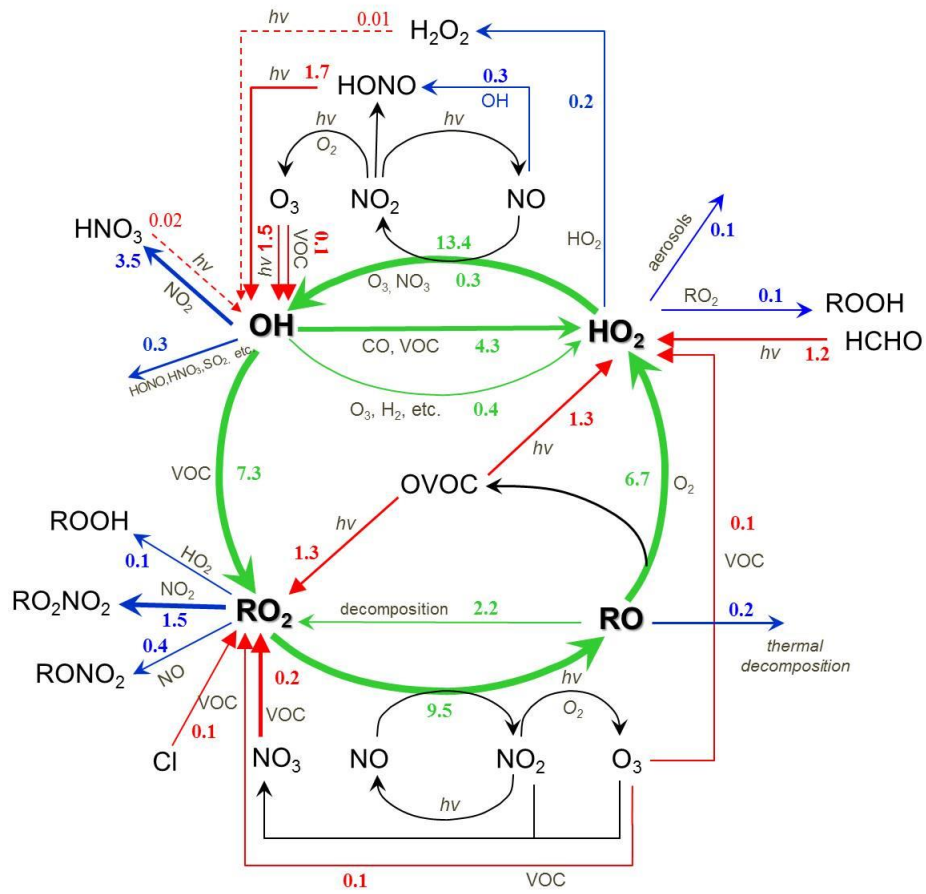
Figure 7. The same as Figure 5 but for the case of 31 August 2011.
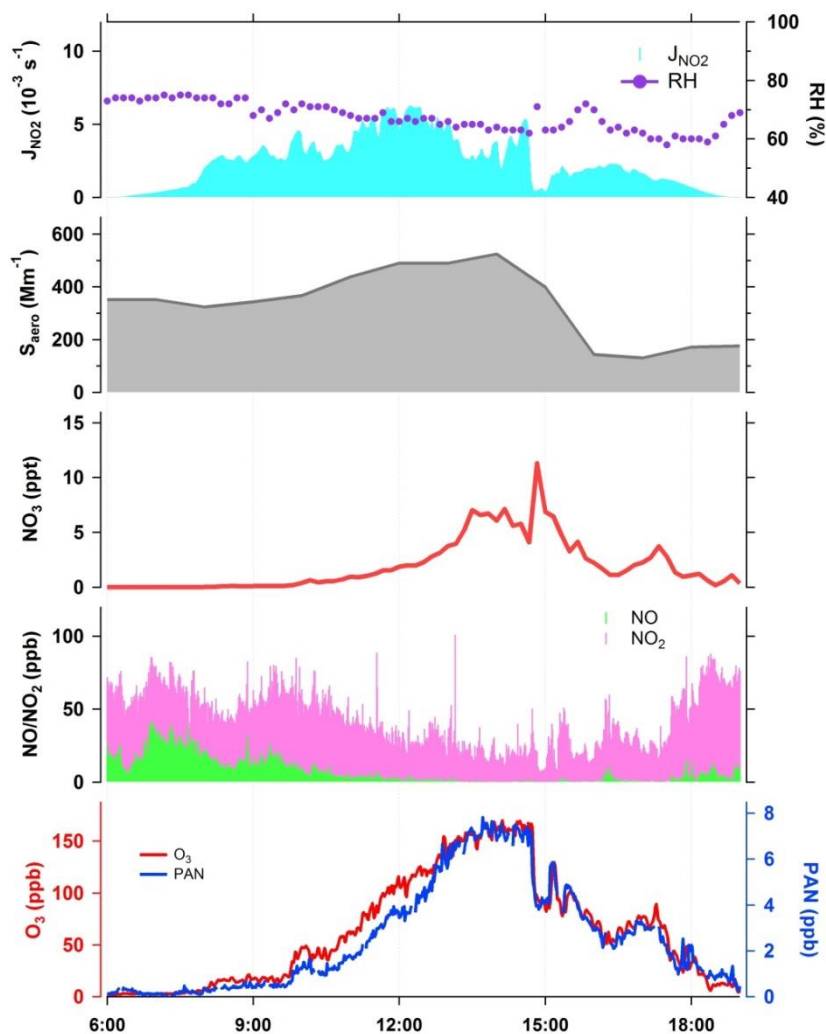
Figure 8. Time series of chemical and meteorological parameters observed at Tung Chung on 25 August 2011.
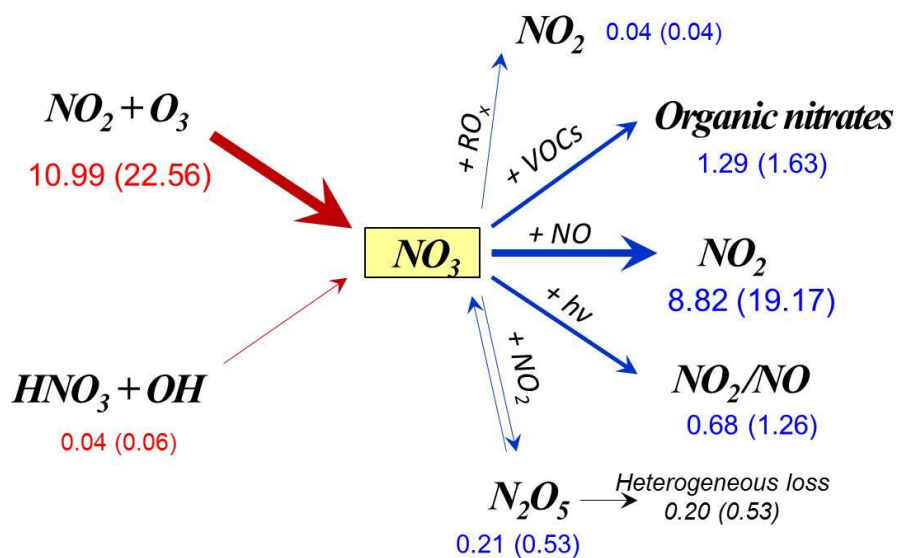
Figure 9. Midday average (9:00–15:00 local time) budget of the NO$_3$ radical at Tung Chung on 25 August 2011. The units are ppb/h. Peak values are also given in parentheses.